Theoretical Study of the Interaction between Methyl Fluoride, Methyl Chloride, and Methyl Bromide with Hydrogen Peroxide

Hue Minh Thi Nguyen, Minh Tho Nguyen, Jozef Peeters, and Thérèse Zeegers-Huyskens*

Department of Chemistry, University of Leuven, 200F Celestijnenlaan, B-3001 Leuven, Belgium

Received: May 31, 2004; In Final Form: September 28, 2004

MP2/6-31+G(d,p) calculations are used to analyze the interaction between CH_3X (X = F, Cl, or Br) and hydrogen peroxide (HP). Two stable structures, A and B, are found on each potential energy surface. The A complexes are characterized by a six-membered structure and the B complexes, having a lower stability, by a five-membered structure. In both complexes, the molecules are held together by both OH···X and CH1···O hydrogen bonds. The binding energies range between 2.0 and 3.2 kcal mol^{-1} for the A complexes and between 1.5 and 1.7 kcal mol^{-1} for the B complexes. The frequency shifts are calculated for the CH1D2D3X isotopomers. Both A and B complexes exhibit simultaneously an elongation of the OH bond and a red shift and an infrared intensity increase of the corresponding OH stretching vibration along with a contraction of the CH1 bond, a blue shift, and an infrared intensity decrease of the CH1 stretching vibration. The interaction of CH_3F and CH_3Cl with HP also induces a contraction of the external CH2 and CH3 bonds and a blue shift of the corresponding stretching vibrations. The results of an NBO analysis are discussed in terms of the hyperconjugation and rehybridization model. While there is a charge transfer from CH_3X to HP in the A complexes, the charge transfer is negligible in the B complexes. Complex formation results in an increase of the occupation of the σ^*(OH) and σ^*(CH1) antibonding orbitals and an increase of the s-character of the corresponding O or C atoms. In contrast, there is a decrease in the occupation of the σ^*(CH2) and σ^*(CH3) orbitals. The n(X) → σ^*(OH) hyperconjugative energies are equal to ∼10 kcal mol^{-1}, and the n(O) → σ^*(CH) hyperconjugative energies range between 1.4 and 2.5 kcal mol^{-1} for the A complexes. Our results show that the OH bond lengths are mainly determined by the occupation of the σ^*(OH) orbitals. The CH distances depend on both the occupation of the σ^*(CH) orbitals and the hybridization of the corresponding C atom.

Introduction

It is increasingly recognized that hydrogen bonds involving CH groups play a crucial role in determining molecular conformation and crystal packing,[1] supramolecular architecture,[2] and the structure of biological systems such as nucleic acids.[3] Much of the evidence of CH···B interactions stems from the observation of close H···B contacts in crystal structures.[4] The formation of standard AH···B hydrogen bonds is accompanied by a small elongation of the AH bond, manifested by a red shift of the AH stretching frequency and a substantial increase of its infrared intensity as compared to the noninteracting species. In the case of CH···B interactions involving C(sp) or C(sp^2), an elongation of the CH bond and a red shift of the corresponding CH stretching vibrations have been observed.[5] For the hydrogen bonds involving these CH groups, the CH stretching frequencies are correlated to the internuclear C···O distances[1j] similarly to the relations found for conventional hydrogen bonds involving OH, NH, and SH proton donor groups.

However, there is a rather limited number of systems where the CH···O interactions result in a *blue shift of the relevant CH stretching vibration*. This has already been observed, more than 20 years ago, by Sandorfy and co-workers[6] in the complexes between perfluoroparaffins and diethyl ether or acetone. Blue shifts were also observed for chloroform complexed with weak proton acceptors[7] and more recently in other hydrogen-bonded systems.[8] Recent theoretical studies suggest that blue-shifting hydrogen bonds are not restricted to CH bonds but can also be observed for SiH, PH, and even NH bonds.[9]

Although Hobza et al.[10] referred to these blue-shifting hydrogen bonds as "anti" or "improper" hydrogen bonds, Scheiner et al. have shown in thorough theoretical studies on the interaction between water and fluoromethanes[11a,b] or in the dimers of fluromethanes[11c] that there are no fundamental distinctions between the mechanisms of the formation of improper and normal hydrogen bonds. The formation of both complexes leads to similar changes in the remote part of the hydrogen-bond acceptor. The studies were further extended to the interaction between chloromethanes and water where the occupation of the σ^*(CH) orbital of the CH···O bond was shown to increase upon complex formation.[12] The similar nature of standard and improper hydrogen bonds appears from the calculations of Dannenberg and co-workers[13] who have shown that, at small electric fields, electron density from the hydrogen moves into the CH bond, shortening and strenghtening it. This conclusion is further substantiated by theoretical considerations of Hermansson[14] whose calculations suggested that the reason for the blue shift is the sign of the dipole moment derivative with respect to the stretching coordinate combined with the exchange overlap at moderate and shorter hydrogen-bond distances. Also, it was shown that the effect of an external electric field is such that when the field and dipole moment are parallel, the bond lengthens, as in the case of OH···O. In contrast, when the field and dipole moment are antiparallel, as in the case of CH···O, the bond shortens.[15] The theoretical

10.1021/jp0404044 CCC: $27.50
Published on Web 11/16/2004

data have been critically summarized in a recent paper by Weinhold and co-workers.[16] In an extended study involving numerous CH···B hydrogen bonds, these authors have shown that the AH bond length in AH···B hydrogen-bonded complexes is controlled by a balance between two main factors acting in opposite directions. The AH bond lengthening resulting from the hyperconjugative interaction due to the charge transfer from a lone pair to the σ^*(AH) antibonding orbital is balanced by AH bond shortening due to an increase in the s-character and polarization of the AH bond. When the hyperconjugative interaction is weak and the X-hybrid orbital in the AH bond is able to undergo a sufficient change in hybridization and polarization, rehybridization turns out to dominate, leading to a shortening of the AH bond and thereby a blue shift in the corresponding AH stretching frequency. This is a logical consequence of Bent's rule,[17] which predicts an increase in s-character of the A-hybrid atomic orbital of the AH bond upon AH···B hydrogen-bond formation as H becomes more positively charged during this process.

In the present study, we expand our studies on blue-shifting hydrogen bonds to the interaction between CH_3F, CH_3Cl, and CH_3Br with hydrogen peroxide (HP). Despite the usefulness of HP in many fields[18] such as atmospheric chemistry, photodissociation dynamics, and oxidation reactions, very few studies have been conducted on their interaction with organic molecules. It must be mentioned, however, that theoretical calculations have been carried out on HP complexed with water,[18] hydrogen halides,[19] urea,[20] and the nucleobases adenine[21] and uracil.[22]

The present paper is ordered as follows. The first part deals with the geometrical characteristics and binding energies. In the second part, we discuss some relevant vibrational features. The third part deals with the results of an NBO analysis, more specifically with the NBO charges, the occupation of relevant antibonding orbitals, the changes in hybridization of the C and O atoms, and the hyperconjugative energies. In the last part, quantitative relationships between bond lengths, occupation of antibonding orbitals, and hybridization of the atoms involved in the interaction are presented.

Computational Methods

The geometries of the isolated CH_3X and HP molecules and their complexes were fully optimized at the MP2/6-31+G(d,p) computational level. This method and basis sets also used in other recent works[9a,11a,12,16] adequately describe blue-shifted hydrogen bonds, and it is a reliable treatment for the purpose of our study. Further, it must be stressed that the main objective of this work is not to compute the properties of the complexes at the best computational level but rather to discuss the bonding trends and to compare them with previous data obtained at the same level. The interaction energies were obtained as the difference in energy between the complex, on one hand, and the sum of the isolated monomers, on the other hand. Basis set superposition errors (BSSEs) were corrected by the counterpoise procedure.[23] It is worth stressing that, for these weak interactions, failure to correct the BSSEs would have resulted in erroneous conclusions.[24] Harmonic vibrational frequencies and infrared intensities were calculated at the same level. Charges on individual atoms, populations of molecular orbitals, and coefficients of the hybrid orbitals were obtained by using the natural bond population scheme.[25]

The interaction between filled and vacant orbitals represents the deviation of the molecule from the Lewis structure and can be used as a measure of delocalization, also called hyperconjugation. The hyperconjugative interaction energy can be calculated from the second-order perturbation theory

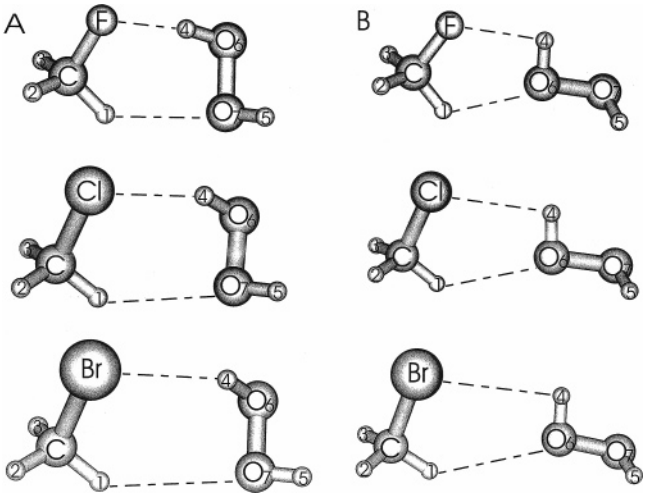

Figure 1. MP2/6-31+G(d,p) geometries of the optimized structures of the A and B complexes between CH_3F, CH_3Cl, and CH_3Br and hydrogen peroxide.

$$E(2) = -n_\sigma \frac{\langle \sigma/F/\sigma^* \rangle^2}{\epsilon_{\sigma^*} - \epsilon_\sigma} = -n_\sigma \frac{F_{ij}^{\ 2}}{\Delta E} \qquad (1)$$

where $\langle \sigma/F/\sigma^* \rangle$, or F_{ij}, is the Fock matrix element between the NBO orbitals i and j, ϵ_σ and ϵ_{σ^*} are the energies of the σ and σ^* NBOs, and n_σ is the population of the donor n orbital. The GAUSSIAN 98 package of programs was used for all calculations reported in the present work.[26]

Results and Discussion

1. Molecular Structure and Binding Energies. For each CH_3X−HP complex, two stable structures are found on the potential energy surface (Figure 1). Both structures are cyclic with two distinct hydrogen bonds involved in the interaction. All the CH1···O and OH···X intermolecular contacts are shorter than the sum of the van der Waals radii and the corresponding angles larger than 90°. In the six-membered A structures, both O atoms of HP are involved in the interaction; in the five-membered B structures, one of the OH groups of HP acts as a proton donor and proton acceptor. It should be mentioned that the CH_3F−HP complex can also adopt an open configuration where the two molecules are held together by one CH1···O hydrogen bond (H1···O distance of 2.675 Å). This complex is characterized by a lower stability and will not be discussed hereafter. All the other possible arrangements and other ring structures are unstable and characterized by one or more imaginary frequencies.

Selected geometrical characteristics for isolated CH_3F, CH_3Cl, CH_3Br, and HP and the A and B complexes are summarized in Table 1. Inspection of this table indicates that the interaction between CH_3X and HP results in a small contraction of the CH1 groups bonded to the O atom of HP. In the A complexes, the contraction ranges between 0.0002 and 0.0018 Å. The contraction of the CH1 bond is smaller in the B complexes and ranges between 0.0004 and 0.0008 Å. Interestingly, in the CH_3F and CH_3Cl complexes, interaction with HP also induces a small contraction of 0.0001−0.0011 Å of the external CH2 and CH3 bonds.

In all the complexes considered, the CX distances increase with respect to the free molecules. This increase is the largest

TABLE 1: Selected Optimized Geometrical Parameters in Free CH_3X and HP and the A and B CH_3X−HP Complexes (Distances in Å, Angles in deg)

free CH_3F and HP			CH_3F−HP (A)	CH_3F−HP (B)
r(CH)	1.0866	Δ*r*(CH1)	−0.018	−0.008
		Δ*r*(CH2)	−0.012	−0.004
		Δ*r*(CH3)	−0.0011	−0.0002
r(CF)	1.4048	Δ*r*(CF)	+0.0152	+0.0096
OH	0.9704	O6H4	+0.0046	+0.0005
OO	1.4726	O6O7	+0.0001	−0.0006
α(HOOH)	121.3	Δα(H4O6O7H5)	−3.9	−5.4

Intermolecular Parameters

CH_3F−HP (A)		CH_3F−HP (B)	
H1···O7	2.556	H1···O6	2.469
CH1O7	127.6	CH1O6	114.7
H4···F	1.909	H4···F	2.418
O7H4F	160.2	O6H4F	98.6

free CH_3Cl or HP			CH_3Cl (A)	CH_3Cl (B)
r(CH)	1.0847	Δ*r*(CH1)	−0.0009	−0.0005
		Δ*r*(CH2)	−0.0004	−0.0001
		Δ*r*(CH3)	−0.0003	−0.0001
r(CCl)	1.7778	Δ*r*(CCl)	+0.0079	+0.0096
r(OH)	0.9704	Δ*r*(O6H4)	+0.0042	+0.0011
r(OO)	1.4726	Δ*r*(O6O7)	−0.0014	−0.0026
α(HOOH)	121.3	Δα(H4O6O7H5)	−7.4	−5.0

Intermolecular Parameters

CH_3Cl−HP (A)		CH_3Cl−HP (B)	
H1···O7	2.450	H1···O6	2.462
CH1O7	137.0	CH1O6	129.0
H4···Cl	2.378	H4···Cl	2.734
OH4Cl	158.2	OH4Cl	110.9

free CH_3Br and HP			CH_3Br−HP (A)	CH_3Br−HP (B)
r(CH)	1.0835	Δ*r*(CH1)	−0.0005	−0.0004
		Δ*r*(CH2)	0.0000	+0.0002
		Δ*r*(CH3)	+0.0002	+0.0002
r(CBr)	1.9470	Δ*r*(CBr)	+0.0076	+0.0066
r(OH)	0.9704	Δ*r*(O6H4)	+0.0051	+0.0008
r(OO)	1.4726	Δ*r*(O6O7)	−0.0011	−0.0027
α(HOOH)	121.3	Δα(H4O6O7H5)	−8.2	−6.4

Intermolecular Parameters

CH_3Br−HP (A)		CH_3Br−HP (B)	
H1···O7	2.431	H1···O6	2.430
CH1O7	137.1	CH1O6	130.3
H4···Br	2.526	H4···Br	2.896
OH4Br	157.4	OH4Br	108.0

in the CH_3F−HP (A) complex (0.0152 Å) and the smallest in the CH_3Br−HP (B) complex (0.0066 Å). A very small variation of the CHX angle is also predicted. We must notice that the elongation of the CX bond seems to be a general feature of the methyl halide complexes. Calculations carried out at the same level have indeed shown that, in the cyclic five-membered CH_3F−H_2O complex, the CF bond is elongated by 0.0124 Å.[12] In contrast, the contraction of the external CH bonds is not a general property of the methyl halide complexes. In the aforementioned system, the external CH bonds are elongated by 0.001 Å.[12]

As expected, complex formation also results in geometrical changes in the HP molecule. The bonded OH4 group is elongated by 0.0042−0.0051 Å in the A complexes and by 0.0005−0.0011 Å in the B complexes. The two OOH angles increase by very small amounts (0.3−1.2°). Larger variations are predicted for the H4O6O7H9 dihedral angle which decreases by a few degrees in all the structures.

TABLE 2: Binding Energies (kcal mol^{-1}) Including BSSE and ZPE Corrections (in Parentheses) for the Interaction between CH_3F, CH_3Cl, and CH_3Br and HP

system	A structure	B structure
CH_3F−HP	−4.65 (−3.24)	−2.80 (−1.74)
CH_3Cl−HP	−4.10 (−2.01)	−3.24 (−1.53)
CH_3Br	−4.44 (−2.39)	−4.22 (−1.64)

The H1···O intermolecular distances decrease from 2.556 to 2.431 Å (A complexes) and from 2.469 to 2.430 Å (B complexes) upon going from CH_3F to CH_3Br. The H4···X distances range from 1.909 to 2.526 Å in the A complexes; they are markedly longer in the B complexes, varying from 2.418 to 2.896 Å.

The binding energies for the A and B complexes including ZPE and BSSE corrections are reported in Table 2. Our results indicate that the binding energies are consistently larger for the A than for the B complexes. This can be accounted for by a larger departure from linearity in the five-membered structures.

Further, it must be mentioned that the OH···X angles ranging from 98 to 110° represent the limit for existence of a hydrogen bond. It is indeed generally accepted that the donor−acceptor bond angle must amount to at least 90°. The binding energies for the B complexes are relatively small and vary in a small range, from −1.53 to −1.74 kcal mol^{-1}. For the A complexes, the binding energies are ordered as follows: $CH_3F > CH_3Br > CH_3Cl$. This ordering results from two different contributions which act in opposite directions.

The values of the intermolecular H1···O distances which decrease from CH_3Br to CH_3F suggest that the strength of the H1···O hydrogen bond is ordered as follows: $CH_3Br > CH_3Cl > CH_3F$, in agreement with the acidity of the CH bonds. Their deprotonation energies are indeed equal to 408.7 (CH_3F), 395.6 (CH_3Cl), and 391.7 (CH_3Br) kcal mol^{-1}.[27] Recent data have also shown that the binding energies of methyl halides with X^- anions follow the order of acidity of the CH bonds.[28] The contractions of the H···X distances with respect to the sum of the van der Waals radii are equal to 0.69 (CH_3F), 0.57 (CH_3Cl), and 0.52 Å (CH_3Br). These data suggest that the H···F bond may be stronger than the H···Cl and H···Br ones. This is consistent with the larger charge on the F atom than that on the Cl or Br atom (see section 3) which results in a greater electrostatic interaction in the OH···F hydrogen bond than in the OH···Cl or OH···Br hydrogen bonds. There is no correlation between the binding energies and the contraction of the CH bond. This results from the fact that, as previously mentioned, the binding energies are the sum of two contributions which act in opposite directions.

It is interesting to compare the present results with the structures and energies of the prereaction adducts of the hydrogen abstraction of OH$^\bullet$ radicals with halogenomethanes calculated at the HF/6-31G(d,p) level.[29] The HO$^\bullet$···HCH_2Cl adduct is found to be more stable than the OH$^\bullet$···$ClCH_3$ one, but the OH$^\bullet$···FCH_3 adduct is more stable by 3.2 kcal mol^{-1} than the HO$^\bullet$···HCH_2F one.

As in the case of the halomethanes and water complexes,[12] we were not able to find a correlation between the CH1 bond lengths and the H1···O distances. This can be accounted for by the fact that the CH1 bond lengths are determined by different factors which act in opposite directions. This will be discussed in the third section of our work.

2. Vibrational Frequencies and Infrared Intensities. The harmonic vibrational frequencies and infrared intensities of selected vibrational modes are reported in Table 3.

Let us discuss at first the stretching vibrations or the different CH bonds which show interesting features. In free CH_3F having C_{3v} symmetry, the E mode is predicted at 3259 cm^{-1} with an infrared intensity of 26 km mol^{-1} and the A1 mode is calculated at 3157 cm^{-1} with an infrared intensity of 33 km mol^{-1}. In the CH_3F−HP (A) complex where the C_{3v} symmetry is lost, the E vibration is split into two components at 3288 and 3278 cm^{-1} with respective infrared intensities of 6 and 18 km mol^{-1}and the low frequency mode is calculated at 3143 cm^{-1} with an infrared intensity of 31 km mol^{-1}. To avoid vibrational coupling between the $\nu(CH_3)$ modes, the frequencies have been calculated in the CH1D2D3X isotopomers. In isolated CH1D2D3F, the ν(CH1) vibration is predicted at 3225 cm^{-1} with an infrared intensity of 28 km mol^{-1}. The largest blue shift of 30 cm^{-1} is calculated in the CH_3F−HP (A) system. This blue shift parallels a large infrared intensity loss of 20 km mol^{-1}. In the two CH_3Cl−HP and CH_3Br−HP complexes, the νCH1 vibrations are blue-shifted by smaller amounts, ranging from 11 to 18 cm^{-1}. The corresponding infrared intensities are also predicted to decrease. The perturbations of the stretching vibrations of the external CH2 and CH3 groups are also worth mentioning. In free CH1D2D3F, the ν^{as}CD2D3 and ν^{s}CD2D3 vibrations are predicted at 2422 and 2301 cm^{-1} with infrared intensities of 18 and 24 km mol^{-1}, respectively. In the CH_3F−HP complex (A), these vibrations are blue-shifted by 12 and 10 cm^{-1}, and the corresponding infrared intensities decrease, taking values between 13 and 22 km mol^{-1}. The ν^{as}CD2D3 and ν^{s}CD2D3 vibrations undergo very small blue shifts in the two CH_3Cl−HP complexes (4 and 3 cm^{-1}) and remain practically unchanged in the two CH_3Br−HP complexes, in agreement with the very small variations of the corresponding CH2 and CH3 distances. It is also worth mentioning that the infrared intensity of the ν^{as}CD2D3 mode increases in both CH_3Br−HP complexes, in contrast with the predictions in other systems.

The results summarized in Table 3 indicate that the νOH vibrations of the bonded O6H4···X group are red-shifted by 70−93 cm^{-1} in the A complexes. In these systems, the infrared intensities of the νOH4 vibrations markedly increase upon complex formation. Much smaller frequency shifts of the νO4H6 vibration are calculated for the B complexes, in agreement with the much smaller elongations of the OH bonds in these structures. In the CH_3F−HP (B) complex, where the ν^{as}OH and ν^{s}OH vibrations are coupled, the average shift is equal to zero. The νOH shifts for the two other B complexes are very small, ranging from 5 to 10 cm^{-1}.

The torsional modes of the OH groups are also very sensitive to the interaction with the CH_3X molecules; their frequencies are predicted to increase by 145−192 cm^{-1} in the A complexes and by 61−69 cm^{-1} in the B complexes.

TABLE 3: Harmonic Frequencies (cm^{-1}), Infrared Intensities (km mol^{-1}, in Parentheses), and Assignment of Selected Vibrational Modes in Isolated CH1D2D3F and HP and the A and B CH1D2D3F−HP Complexes

free CH1D2D3F or HP	assignment[a]	CH1D2D3F−HP (A)	CH1D2D3F−HP (B)
3825 (70)	ν^{as}OH	3826 (41) (νOH5)	3821 (39)
3824 (14)	ν^{s}OH	3755 (237) (νOH4)	3829 (56)
3225 (28)	νCH1	3255 (8)	3243 (12)
2422 (18)	ν^{as}CD2D3	2436 (13)	2426 (17)
2301 (24)	ν^{s}CD2D3	2311 (22)	2304 (25)
1077 (63)	νCF[b]	1055 (54)	1062 (62)
905 (0.5)	νOO	906 (2)	905 (1)
372 (235)	τOH	542 (168) (τOH4)	441 (204) (τOH4)
free CH1D2D3Cl or HP	**assignment[a]**	**CH1D2D3Cl−HP (A)**	**CH1D2D3Cl−HP (B)**
3825 (70)	ν^{as}OH	3822 (44) (νOH5)	3820 (42)
3824 (14)	ν^{s}OH	3748 (216) (νOH4)	3814 (57)
3243 (11)	νCH1	3261 (5)	3256 (4)
2434 (3)	ν^{as}CD2D3	2439 (2)	2436 (3)
2315 (15)	ν^{s}CD2D3	2318 (13)	2316 (14)
905 (0.5)	νOO	906 (1)	910 (1)
745 (16)	νCCl	733 (18)	736 (19)
372 (235)	τOH	517 (140) (τOH4)	434 (189) (τOH4)
free CH1D2D3Br or HP	**assignment[a]**	**CH1D2D3Br−HP (A)**	**CH1D2D3Br−HP (B)**
3825 (70)	ν^{as}OH	3821 (45) (νOH5)	3819 (44)
3824 (14)	ν^{s}OH	3731 (236) (νOH4)	3818 (47)
3260 (6)	νCH1	3271 (5)	3272
2448 (1)	ν^{as}CD2D3	2451 (8)	2449 (8)
2322 (10)	ν^{s}CD2D3	2321 (8)	2320 (10)
905 (0.5)	νOO	905 (1)	907 (1)
600 (8)	νCBr[b]	595 (5)	593 (10)
372 (235)	τOH	564 (133)	433 (178)

[a] ν, stretching vibration; τ, torsional vibration. [b] Coupled with the rocking mode of the CD2D3 group.

The data obtained in this work allow us to establish correlations between the frequency shifts of the stretching vibrations and the variations of the corresponding bond lengths.

For the CH1 bond involved in complex formation, the following relationship is obtained:

$$\Delta\nu(\mathrm{CH1})\ (\mathrm{cm}^{-1}) = 7.1 - (12.8 \times 10^3)\Delta r(\mathrm{CH1})\ (\text{Å}) \quad (r = 0.9977) \quad (2)$$

Notice that this correlation has been obtained from the blue shifts and the contraction of the CH1 bond, in contrast with conventional AH···B hydrogen bonds where the $\Delta\nu - \Delta r$ correlations are obtained from the elongation of the AH bond and the red shift of the corresponding streching frequencies.

The relationship between the frequency shifts of the νO6H4 and νO7H5 vibrations and the elongations of the corresponding OH bonds can be written as

$$\Delta\nu(\mathrm{OH})\ (\mathrm{cm}^{-1}) = -1.2 - (17.2 \times 10^3)\Delta r(\mathrm{OH})\ (\text{Å}) \quad (r = 0.9869) \quad (3)$$

The slopes of eqs 2 and 3 demonstrate the greater sensitivity of the νOH stretching vibrations to variations of the corresponding bond lengths. This may be related to the larger σ-acceptor character of the OH bond.

3. NBO Analysis. The formation of a hydrogen bond implies that a certain amount of electronic charge is transferred from the proton acceptor to the proton donor molecule. In addition, there is a rearrangement of electron density within each monomer. This has been discussed recently for the interaction between fluoromethanes and chloromethanes with water.[12] Table 4 summarizes the results of an NBO analysis for the present systems. This table reports the overall charge transfer (CT) occurring from one molecule to another, the NBO charges, the occupation of the σ^* antibonding orbitals of the CH, CX, and OH bonds, and the percentage of s-character of selected bonds in the isolated CH_3X and HP molecules and in their complexes. This table also contains the energies of the hyperconjugative interactions $n(\mathrm{X}) \rightarrow \sigma^*(\mathrm{O4H6})$ and $n(\mathrm{O}) \rightarrow \sigma^*(\mathrm{CH1})$.

Inspection of these results shows that the charge transfer (CT) occurs from CH_3X to HP in the A complexes. The CT ranges from 0.0103 to 0.0157 e. In contrast, the CT is negligible (sligthly positive or negative) in the B complexes. This indicates that, in these systems, the two partners are held together by intramolecular polarization. We may also note that the amount of CT does not exactly match the sum of changes of the population of bonding and antibonding orbitals. The small difference can be rationalized in terms of a small variation of the occupation of the Rydberg orbitals. In the CH_3F−HP (A) complex, for example, the occupation of the Rydberg orbital on the C atom decreases by 0.0004 e and the occupation of the Rydberg orbitals on the F, O4, and H5 atoms increases by 0.0007, 0.0002, and 0.0009 e, respectively.

We will now discuss more in detail the results of the NBO analysis for the CH bonds which is one of the main objectives of our work. A common property of all the systems is the decrease of electronic charge on the bridging proton H1. This decrease ranges between 0.021 and 0.024 e in the A complexes and is somewat smaller in the B complexes, ∼0.0180 e. In the two CH_3F−HP complexes, the C atom gains electronic charge, leading to an increased $C^-\ H1^+$ polarization. In the two CH_3Cl−HP and CH_3Br−HP complexes, the C atoms lose electronic charge. It is noteworthy that, in agreement with Bent's rule, the decrease of electronic charge on H1 parallels an increase of the percentage of s-character of the C bonded to H1. In the isolated molecules, the percentage of s-character of the CH1 bond is equal to 26.9% (CH_3F and CH_3Cl) and 27.5% (CH_3Br). In the complexes, the s-character increases slightly, taking values of 27.6−27.7% in the CH_3F and CH_3Cl adducts and having a maximal value of 28.4% in the CH_3Br−HP (A) complex. A very important result of the NBO analysis is that, in all the systems examined, complex formation results in an *increase* of the occupation of the σ^*CH1 orbital. This increase amounts to 0.0002−0.0009 e in the CH_3F−HP adduct, 0.0018−0.0019 e in the CH_3Cl−HP complex, and 0.0023 e in the CH_3Br−HP complex. Our results also show that the hyperconjugative energies n(O6) or n(O7) → σ^*(CH1) are moderate, ranging from 1.4 to 2.5 kcal mol^{-1} for the A complexes and from 0.8 to 1.9 kcal mol^{-1} for the B complexes.

The variations of charge and hybridization on the external CH2 and CH3 bonds of the systems are also worth mentioning. In the A complexes, we note a small decrease of electronic charge on H2 and a very small increase in the B complexes. The percentage of s-character of the C atom bonded to the H2 or H3 atoms does not change markedly. In contrast with the CH1 bonds, the occupation of the σ^*CH2 orbital *decreases* slightly in all the systems, by amounts ranging from 0.000 47 to 0.0014 e.

As claimed in ref 30, a key difference between the blue- and red-shifting hydrogen bonds may be the target of the charge transfer. Although for red-shifting hydrogen bonds it is a σ^* antibonding orbital, for blue-shifting hydrogen bonds, it is the remote part of the proton acceptor. These conclusions are valuable for complexes involving F_3CH and proton acceptors, where the electonegativity of the F atom causes an electronic flow in the remote part of the system. However, in the present complexes, our results clearly show that there is an increase in the σ^* population of the CX and CH1 bonds involved in the interaction and that there is no appreciable charge transfer to the remote part of the complexes, with the variations of electronic charge on the H2 and H3 atoms being very small and the population of the σ^*(CH2) or σ^*(CH3) antibonding orbitals decreasing slightly.

Let us now discuss the changes occurring in the HP molecule upon complexation. A common feature of all the complexes is the marked decrease of the electronic charge on the bridging proton H4, ranging from 0.001 96 to 0.0235 e, and the increase of the electronic charge on the O6 atom, ranging from 0.0039 to 0.0215 e in the A complexes. This leads to an increasing $O6^-\ H4^+$ polarity similar to the conventional hydrogen bonds. The occupation of the σ^*(OH) orbital is 0.002 55 e in free HP; this occupation takes values of ∼0.017−0.024 e in the A complexes and ∼0.003−0.006 e in the B complexes. These changes parallel an increase of the percentage of s-character of O6 bonded to H4 which is equal to 23.8% in free HP and increases to 26.3−26.6% in the A complexes. This is again in agreement with Bent's rule. Smaller changes are predicted for the B complexes where the percentage of s-character of O6 bonded to H4 ranges between 24.6 and 24.9%. Smaller variations are calculated for the external H5 atom, with the charge on this atom decreasing sligthly in the A complexes and increasing slightly in the B complexes

We must also note that the hyperconjugative energies n(X) → σ^*(OH) calculated according to eq 1 are relatively large in the A complexes, ranging from 9.9 to 10.2 kcal mol^{-1}. They are much smaller in the B complexes, ranging from 0.5 to 1.9 kcal mol^{-1}.

4. Correlation between Bond Lengths, Occupation of the Antibonding Orbitals, and Hybridization. As discussed in a

TABLE 4: NBO Analysis of the A and B CH_3X−HP Complexes−NBO Charges (e), CT (e), Occupation of Antibonding Orbitals (e), % s-Character, and Hyperconjugative Energies (kcal mol^{-1})

	free CH_3F or HP		CH_3F−HP (A)	CH_3F−HP (B)
NBO charge	−0.1154	C	−0.1236	−0.1191
C				
H	0.1890	H1	0.2130	0.2073
		H2	0.1946	0.1869
		H3	0.1933	0.1892
F	−0.4517	F	−0.4671	−0.4650
O	−0.5112	O6	−0.5347	−0.5174
H	0.5112	H4	0.5327	0.5253
CT			0.0103	−0.0007[a]
σ*(CH)	0.01064	σ*(CH1)	0.01086	0.01158
		σ*(CH2)	0.00921	0.00996
		σ*(CH3)	0.00928	0.01006
σ*(CF)	0.00397	σ*(CF)	0.00502	0.00452
σ*(OH)	0.00255	σ*(OH4)	0.01736	0.00366
		σ*(OH5)	0.00259	0.00275
% s-character	26.9	C at H1	27.7	27.5
C at H				
		C at H2 (H3)	27.0	26.8
C at F	19.4	C at F	18.4	18.9
O at H	23.8	O6 at H4	26.8	24.6
		O6 (O7) at H5	23.9	23.6
	LP(1)(F) to σ*(O4H6)		10.1	0.6
	LP(2)(F) to σ*(O4H6)		1.6	0.8
	LP(1)(O6)(O7) to σ*(CH1)		1.4	0.6
	LP(2) (O6)(O7) to σ*(CH1)		0.4	0.8

	free CH_3Cl or HP		CH_3Cl−HP (A)	CH_3Cl−HP (B)
NBO charge	−0.6325	C	−0.6263	−0.6269
C				
H	0.2440	H1	0.2660	0.2617
		H2	0.2447	0.2433
		H3	0.2460	0.2433
Cl	−0.0994	Cl	−0.1155	−0.1193
O	−0.5112	O6	−0.5311	−0.5242
H	0.5112	H4	0.5167	0.5220
CT			+0.0149	+0.0018
σ*(CH)	0.00965	σ*(CH1)	0.01151	0.01140
		σ*(CH2)	0.00876	0.00900
		σ*(CH3)	0.00872	0.00900
σ*(CCl)	0.00145	σ*(CCl)	0.00168	0.00161
σ*(OH)	0.00255	σ*(OH4)	0.01960	0.00637
		σ*(OH5)	0.00268	0.00271
% s-character	26.9	C at H1	27.9	27.6
C at H				
		C at H2 (H3)	26.9	26.8
C at Cl	19.4	C at Cl	18.4	18.7
O at H	23.8	O6 at H4	26.5	24.9
		O7 (O6) at H5	24.0	23.7
	LP(1)(Cl) to σ*(O4H4)		10.2	1.9
	LP(2)(Cl) to σ*(O4H6)		0.7	0.3
	LP(1)(O6)(O7) to σ*(CH1)		2.5	1.6
	LP(2)(O6)(O7) to σ*(CH1)		*b*	0.4

	free CH_3Br or HP		CH_3Br−HP (A)	CH_3Br−HP (B)
NBO charge	−0.7053	C	−0.6947	−0.6946
C				
H	0.2511	H1	0.2725	0.2699
		H2	0.2535	0.2486
		H3	0.2507	0.2496
Br	−0.04805	Br	−0.0666	−0.0715
O	−0.5112	O6	−0.5308	−0.5229
H	0.5112	H4	0.5151	0.5218
CT			0.0157	0.0019
σ*(CH)	0.00725	σ*(CH1)	0.00955	0.00958
		σ*(CH2)	0.00661	0.00678
		σ*(CH3)	0.00671	0.00675
σ*(CBr)	0.00186	σ*(CBr)	0.00212	0.00205
σ*(OH)	0.00255	σ*(OH4)	0.02400	0.00589
		σ*(OH5)	0.00268	0.00277
% s-character	27.5	C at H1	28.4	28.3
C at H				
		C at H2 (H3)	27.4	27.4
C at Br	17.6	C at Br	16.7	16.9
O at H	23.8	O6 at H4	26.3	24.8
		O7 (O6) at H5	24.0	23.7
	LP(1)(Br) to σ*(O4H6)		9.9	1.6
	LP(2)(Br) to σ*(O4H6)		0.5	0.2
	LP(1)(O6)(O7) to σ*(CH1)		2.4	1.9
	LP(2)(O6)(O7) to σ*(CH1)		*b*	0.5

[a] Charge transfer from HP to CH_3F. [b] Lower than 0.05 kcal mol^{-1}.

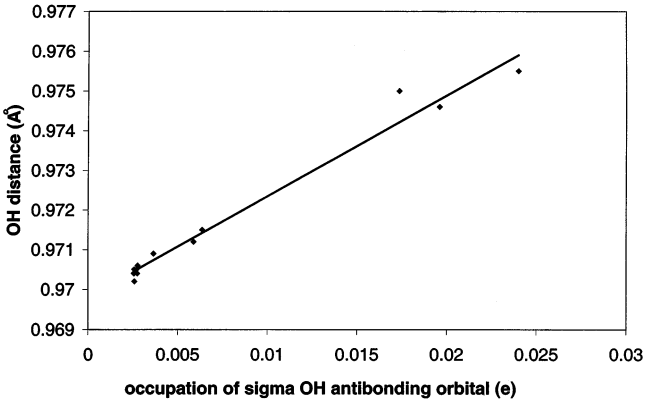

Figure 2. r(OH) (Å) as a function of the occupation of the σ^*(OH) antibonding orbital (e).

recent work,[16] the AH bond length in AH···B hydrogen-bonded complexes is controlled by a balance of two main factors acting in opposite directions. The AH bond lengthening due to the $n \rightarrow \sigma^*$(AH) hyperconjugative interaction is balanced by AH bond shortening due to the increase in s-character and polarization of the AH bond. When hyperconjugation is dominant, the AH bond lengthens. When hyperconjugation is weak and the structure of the proton donor allows for a significant change in AH bond hybridization, the AH bond shortens.

Let us now discuss how both factors are influencing the OH and CH bond lengths for the present systems.

As mentioned in the previous sections, complex formation causes a marked increase of the occupation of the σ^*(OH) antibonding orbitals of HP. There is also a small increase (2% or less) of the percentage of s-character of the O atom. Our results show clearly that the first effect *predominates* in determining the OH bond length. Considering all the free and complexed OH bonds of HP, we have deduced the following correlation illustrated in Figure 2:

$$r(\text{OH})\ (\text{Å}) = 0.9698 + 0.2544\sigma^*(\text{OH})\ (\text{e}) \qquad (r = 0.9896) \quad (4)$$

Interestingly, a very similar equation has been recently obtained for the complexes between cytosine tautomers and water where the ν(OH) frequencies vary within a much broader range and the percentage of s-character of the OH bond remains almost constant (23.4−24%).[31]

We must note that the hyperconjugative energies in the A complexes are relatively large but nearly constant (10 kcal mol^{-1}) in such a way that we could not establish a correlation between the hyperconjugative energies and the bond lengths similar to the one reported recently for CHF_3 complexed with a variety of proton acceptors.[16] In the present case, we are comparing the hyperconjugative energies n(X) $\rightarrow \sigma^*$(OH) in the OH···X (X = F, Cl, or Br) hydrogen bonds which may be influenced by the nature of the methyl halide. Our calculations indicate that the energies of the valence lone pairs of the halogen are not the same, decreasing from CH_3F to CH_3Br. As a consequence, the occupation of the σ^*(OH) (or σ^*(CH)) orbitals in the complexes may be more relevant than the hyperconjugative energies.

We will discuss now the factors influencing the CH bond lengths. In the CH_3F−HP and CH_3Cl−HP systems, the hybridization of the C bonded to the external H2 or H3 atoms remains almost constant. For a nearly constant percentage of s-character of the C atom, the CH bond lengths are mainly determined by the *occupation of the corresponding σ*(CH) orbitals*. Inversely,

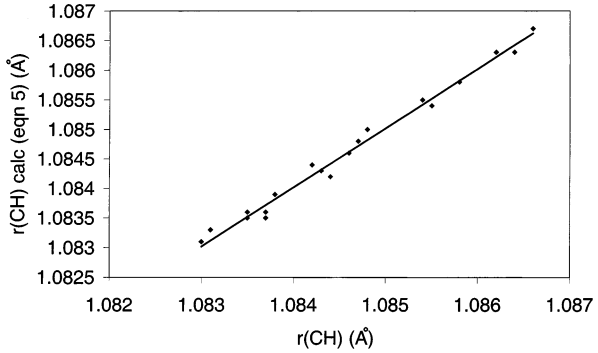

Figure 3. CH bond lengths calculated by eq 5 as a function of the theoretical CH bond lengths (Å).

for systems characterized by a nearly constant occupation of the σ^*(CH) orbital, the CH bond lengths are mainly determined by the percentage of *s-character* of the considered atom. For each isolated CH_3X molecule and its A and B complexes (n = 7), we have derived the following dual expression:

$$r(\text{CH}) = A - 0.0020(\text{s-character of the CH bond (\%)}) + 0.0060\sigma^*(\text{CH}) \quad (5)$$

where σ^*(CH) is expressed in electronic fraction, to have dimensionless units. The A values are values are equal to 1.1339 Å for the CH_3F systems, 1.1328 Å for the CH_3Cl systems, and 1.1348 Å for the CH_3Br systems. Equation 5 allows one to predict CH values with a deviation of ±0.0001 Å for the CH_3F systems and ±0.0002 Å for the CH_3Cl and CH_3Br systems. The correlation between the CH bond lengths predicted by eq 5 and the theoretical CH distances is shown in Figure 3 (correlation coefficient 0.9929). We note that the coefficient of s-character is between the value of −0.0014 and −0.0026 calculated in ref 16. Further, eq 5 has been tested for the CHF_3 complexes (the proton acceptors are H_2O, FH, oxirane, Me_2O, Cl^-, and NH_3), calculated at the same level of theory.[16] In this case, the correlation coefficient is only 0.9775 and much larger deviations are obtained for the H_2S and ClH complexes. This suggests that the coefficients of eq 5 depend not only on the nature of the proton donor but also on the nature of the proton acceptor.

It should be further mentioned that complex formation results in an increase of the C−X distances in all the systems. This bond lengthening is related to the increase of the occupation of the σ^*(CX) orbitals and to the decrease of the percentage of s-character of the C bonded to the halogen atoms, with both effects contributing to the elongation of the CX bonds. The effects are the largest fot the CH_3F (A) complex, where the σ^*(CF) occupation increases by ∼0.001 e and the percentage of s-character of C bonded to F increases by 1%. We note that in the CH_3F/CHF_3 dimer, where the CF distance elongates by 0.008 Å, the σ^*(CF) occupation increases by a smaller amount (0.0006 e).[11c] The variation of hybridization of C bonded to F was not reported.

Finally, theoretical results obtained recently for the first local minimum of the cyclic formic acid dimer are worth mentioning.[32] In this structure, OH···O and CH···O hydrogen bonds are involved in the formation of the closed complex. The contraction of the CH bond parallels a decrease of the occupation of the σ^*(CH) orbital and an increase of the s-character of the C atom. A reverse trend is predicted for the nonbonded CH bond (elongation, increase of the occupation of σ^*(CH), and decrease of the s-character of the C atom). For these two bonds, both effects are acting in the same direction. This is no more the case for the two external CH bonds in the conventional dimer

where the molecules are held together by two OH···O hydrogen bonds. In this centrosymmetrical dimer, the two external CH bonds are slightly contracted and there is a decrease of the σ^*-(CH) occupation and of the s-character of the C atom. Both effects are acting in opposite directions, but this does not contradict the rehybridization model, as demonstrated in the present work. The number of theoretical data dealing with the formic acid dimers do not allow quantitative correlations similar to those deduced in the present work to be established.

Concluding Remarks

The present work deals with theoretical calculations of the interaction between methyl halides, CH_3X, and hydrogen peroxide. Two stable structures involving the formation of a six-membered or five-membered ring are found on the potential energy surface. In both structures, the molecules are held together by OH···X and CH1···O hydrogen bonds. The complexes exhibit simultaneously an elongation of the OH bond and a red shift of the ν(OH) vibration along with a contraction of the CH1 bond and a blue shift of the ν(CH1) vibration. The external CH2 and CH3 bonds also show interesting geometrical and vibrational features. The most important results emerging from our calculations are the relationships between the OH and CH bond lengths, the occupation of the corresponding antibonding orbitals, and the hybridization of the O or C bonded to the H atoms.

Acknowledgment. M.T.N., J.P., and H.M.T.N. thank the KULeuven Research Council for continuing support (GOA-program and doctoral fellowship).

References and Notes

(1) (a) Green, R. D. *Hydrogen Bonding by CH groups*; MacMillan: London, 1974. (b) Wiberg, K. B.; Waldon, R. F.; Schulte, G.; Saunders, M. *J. Am. Chem. Soc.* **1991**, *113*, 971. (c) Desiraju, R. *J. Chem. Soc., Chem. Commun.* **1990**, 454. (d) Steiner, T.; Saenger, W. *J. Am. Chem. Soc.* **1992**, *114*, 10146. (e) Steiner, T.; Saenger, W. *Acta Crystallogr.* **1992**, *B48*, 819. (f) Steiner, T. *Crystallogr. Rev.* **1996**, *6*, 1. (g) Chaney, J. D.; Goss, C. R.; Folting, B. D.; Santarsiero, B. D.; Hollingsworth, M. D. *J. Am. Chem. Soc.* **1996**, *118*, 9432. (h) Steiner, T.; Kanters, J. A.; Kroon, J. *Chem. Commun.* **1996**, 1277. (i) Kariuki, B. M.; Harris, K. M. D.; Philip, D.; Robinson, J. M. A. *J. Am. Chem. Soc.* **1997**, *119*, 12679. (j) Desiraju, G. R.; Steiner, T. *The Weak Hydrogen Bond in Structural Chemistry and Biology*; Oxford University Press: Oxford, U.K., 2001. (k) Jeffrey, G. A. *J. Mol. Struct.* **1999**, *485*, 293. (l) Steiner, T. *J. Phys. Chem. A* **2000**, *104*, 1479. (m) Swamy, K. C. K.; Kumaraswamy, S.; Kommana, P. *J. Am. Chem. Soc.* **2001**, *123*, 12642. (n) Ribeiro-Claro, P. J. A.; Drew, M. G. B.; Félix, V. *Chem. Phys. Lett.* **2002**, *356*, 318.

(2) (a) Houk, K. N.; Menzer, S.; Newton, S. P.; Raymo, F. M.; Fraser Stoddart, J.; Williams, D. J. *J. Am. Chem. Soc.* **1999**, *121*, 1479. (b) Mehta, G.; Vidya, R. *J. Org. Chem.* **2000**, *65*, 3497.

(3) (a) Metzger, S.; Lippert, B. *J. Am. Chem. Soc.* **1996**, *118*, 12467. (b) Sigel, R. K. O.; Freisinger, E.; Metzger, S.; Lippert, B. *J. Am. Chem. Soc.* **1998**, *120*, 12000. (c) Hobza, P.; Šponer, J.; Cubero, E.; Orozco, M.; Luque, J. *J. Phys. Chem. B* **2000**, *104*, 6286 and references therein. (d) Hocquet, A.; Ghomi, A. *Phys. Chem. Chem. Phys.* **2000**, *2*, 5351.

(4) Taylor, R. B.; Kennard, O. *J. Am. Chem. Soc.* **1982**, *104*, 5063.

(5) (a) Engdahl, A.; Nelander, B. *Chem. Phys. Lett.* **1983**, *100*, 129. (b) DeLaat, A. M.; Ault, B. S. *J. Am. Chem. Soc.* **1987**, *109*, 4232. (c) Jeng, M.-L.; DeLaat, A. M.; Ault, B. S. *J. Phys. Chem.* **1989**, *93*, 3997.

(6) Trudeau, G.; Dumas, J.-M.; Dupuis, P.; Guérin, M.; Sandorfy, C. *Top. Curr. Chem.* **1980**, *93*, 91.

(7) (a) Budsinsky, M.; Fiedler, A. Z. *Synthesis* **1989**, 858. (b) Boldeskul, I. E.; Tsymbal, I. F.; Ryltsev, E. V.; Latajka, Z.; Barnes, A. J. *J. Mol. Struct.* **1997**, *436*, 167.

(8) (a) Hobza, P.; Spirko, V.; Havlas, Z.; Buchold, K.; Reimann, B.; Barth, H.-D.; Brutschy, B. *Chem. Phys. Lett.* **1999**, *299*, 180. (b) Reimann, B.; Buchold, K.; Vaupel, S.; Brutschy, B.; Havlas, Z.; Hobza, P. *J. Phys. Chem. A* **2001**, *105*, 5560. (c) Dalanoye, S. N.; Herrebout, W. A.; van der Veken, B. J. *J. Am. Chem. Soc.* **2002**, *124*, 11854.

(9) (a) Li, X.; Liu, L.; Schlegel, H. B. *J. Am. Chem. Soc.* **2002**, *124*, 9639. (b) Fang, Y.; Fan, J.-M.; Liu, L.; Li, X.-S.; Guo, Q.-X. *Chem. Lett.* **2002**, 116.

(10) Hobza, P.; Havlas, Z. *Chem. Rev.* **2000**, *100*, 4253.

(11) (a) Gu, Y.; Kar, T.; Scheiner, S. *J. Am. Chem. Soc.* **1999**, *121*, 9411. (b) Scheiner, S.; Kar, T. *J. Phys. Chem. A* **2002**, *106*, 1784. (c) Kryachko, E. K.; Scheiner, S. *J. Phys. Chem. A* **2004**, *108*, 2527.

(12) Kryachko, E. K.; Zeegers-Huyskens, Th. *J. Phys. Chem. A* **2001**, *105*, 7118.

(13) Masunov, A.; Dannenberg, J. J.; Contreras, R. H. *J. Phys. Chem. A* **2001**, *105*, 4737.

(14) Hermansson, K. *J. Phys. Chem. A* **2002**, *106*, 4695.

(15) Qian, W.; Krimm, S. *J. Phys. Chem. A* **2002**, *106*, 6628.

(16) Alabugin, I. V.; Manoharan, M.; Peabody, S.; Weinhold, F. *J. Am. Chem. Soc.* **2003**, *125*, 5973.

(17) Bent, H. A. *Chem. Rev.* **1961**, *61*, 275.

(18) Dobado, J. A.; Molina, J. *J. Phys. Chem.* **1994**, *98*, 1819.

(19) Dobado, J. A.; Molina, J. *J. Phys. Chem.* **1994**, *98*, 7819.

(20) Dobado, J. A.; Molina, J.; Portal, D. *J. Phys. Chem. A* **1998**, *102*, 778.

(21) Dobado, J. A.; Molina, J. *J. Phys. Chem. A* **1999**, *103*, 4755.

(22) Wysokiñsky, R.; Michalska, D.; Bieñko, D. C.; Zeegers-Huyskens, Th. *J. Phys. Chem. A* **2003**, *107*, 8730.

(23) Boys, S. F.; Bernardi, F. J. *Mol. Phys.* **1979**, *19*, 553.

(24) Hobza, P.; Spirko, V.; Selzle, H. L.; Schlag, E. W. *J. Phys. Chem. A* **1998**, *102*, 250.

(25) Reed, A. E.; Curtiss, L. A.; Weinhold, F. *Chem. Rev.* **1988**, *88*, 899.

(26) Frisch, M. J.; Trucks, G. W.; Scuseria, G. E.; Robb, M. A.; Cheeseman, J. R.; Zakrzewski, V. G.; Montgomery, J. A., Jr.; Stratmann, R. E.; Burant, J. C.; Dapprich, S.; Millam, J. M.; Daniels, A. D.; Kudin, K. N.; Strain, M. C.; Farkas, O.; Tomasi, J.; Barone, V.; Cossi, M.; Cammi, R.; Mennucci, B.; Adamo, C.; Clifford, S.; Ochterski, J.; Petersson, G. A.; Ayala, P. Y.; Cui, Q.; Morokuma, K.; Malick, D. K.; Rabuck, A. D.; Raghavachari, K.; Foresman, J. B.; Ciolowski, J.; Ortiz, J. V.; Stefavov, B. B.; Liu, G.; Liashenko, A.; Piskorz, P.; Komaromi, I.; Gomperts, R.; Martin, R. L.; Fox, D. J.; Keith, T.; Al-Laham, M. A.; Peng, C. Y.; Nanayakkara, A.; Gonzales, C.; Challacombe, M.; Gill, P. M. W.; Johnson, B. G.; Chen, W.; Wong, M. W.; Andres, J. L.; Head-Gordon, M.; Repogle, E. S.; Pople, J. A. *Gaussian 98*, revision A.5; Gaussian, Inc.: Pittsburgh, PA, 1998.

(27) Lias, S. G.; Bartmess, J. E.; Liebman, J. F.; Holmes, J. L.; Levin, R. D.; Mallard, W. G. *J. Phys. Chem. Ref. Data* **1988**, *17*, Supp. 1.

(28) Parthiban, S.; de Oliviera, G.; Martin, J. M. L. *J. Phys. Chem. A* **2001**, *105*, 895.

(29) El-Taher, S. *Int. J. Quantum Chem.* **2001**, *84*, 426.

(30) Hobza, P. *Phys. Chem. Chem. Phys.* **2001**, *3*, 2555.

(31) Comparison of eqs 3 and 4 allows one to calculate the correlation between the frequency shifts of the ν(OH) stretching vibration and the occupation of the σ^*OH orbitals: $\Delta\nu(\mathrm{OH})\ (\mathrm{cm}^{-1}) = -11 + 4507\sigma^*(\mathrm{OH})$ (e) ($r = 0.9835$). A very similar equation has been recently obtained for the complexes between cytosine tautomers and water (Chandra, A. K.; Michalska, D.; Wysokinsky, R.; Zeegers-Huyskens, Th. *J. Phys. Chem. A*, in press).

(32) Chocholoušová, J.; Špirko, S.; Hobza, P. *Phys. Chem. Chem. Phys.* **2004**, *6*, 37.